Available online at www.sciencedirect.com

ScienceDirect

Current Opinion in Chemical Biology

Structure-based mechanistic insights into catalysis by small self-cleaving ribozymes

Aiming Ren[1], Ronald Micura[2] and Dinshaw J Patel[3]

Small self-cleaving ribozymes are widely distributed in nature and are essential for rolling-circle-based replication of satellite and pathogenic RNAs. Earlier structure–function studies on the hammerhead, hairpin, *glmS*, hepatitis delta virus and Varkud satellite ribozymes have provided insights into their overall architecture, their catalytic active site organization, and the role of nearby nucleobases and hydrated divalent cations in facilitating general acid-base and electrostatic-mediated catalysis. This review focuses on recent structure–function research on active site alignments and catalytic mechanisms of the Rzb hammerhead ribozyme, as well as newly-identified pistol, twister and twister–sister ribozymes. In contrast to an agreed upon mechanistic understanding of self-cleavage by Rzb hammerhead and pistol ribozymes, there exists a divergence of views as to the cleavage site alignments and catalytic mechanisms adopted by twister and twister–sister ribozymes. One approach to resolving this conundrum would be to extend the structural studies from currently available pre-catalytic conformations to their transition state mimic vanadate counterparts for both ribozymes.

Addresses
[1] Life Sciences Institute, Zhejiang University, Hangzhou 310058, China
[2] Institute of Organic Chemistry, Leopold Franzens University, Innsbruck A6020, Austria
[3] Structural Biology Program, Memorial Sloan-Kettering Cancer Center, New York, NY 10065, USA

Corresponding author: Patel, Dinshaw J (pateld@mskcc.org)

Current Opinion in Chemical Biology 2017, **41**:71–83

This review comes from a themed issue on **Mechanistic biology**

Edited by **Gregory A. Weiss**

For a complete overview see the Issue and the Editorial

Available online 3rd November 2017

http://dx.doi.org/10.1016/j.cbpa.2017.09.017

Introduction

RNA has been postulated to play a central role in early life (the RNA world hypothesis), given that both genomic information and enzymatic function reside in the same biological macromolecule. RNA enzymes (ribozymes) are composed of only four nucleotides of a common chemical nature projecting from a negatively-charged ribose-phosphate backbone with the capacity to accelerate cleavage of the phosphodiester backbone by up to 10^6-fold. This raises the issue as to how ribozyme catalysis occurs at neutral pH, given that ionization of nucleobases and riboses only occur under pronounced basic/acidic conditions. The focus of this review will be on recent studies of natural self-cleaving ribozymes, due to their small size and catalytic versatility, thereby offering unprecedented opportunities to understand chemistry in the prebiotic world and its evolution over time to the modern era.

Small self-cleaving ribozymes are widely distributed in nature [1••] and are essential for rolling-circle-based replication of satellite and pathogenic RNAs [2,3] and processing of repetitive RNA species [4]. Current understanding of the various contributions to small self-cleaving ribozyme-mediated rate enhancement has emerged from earlier structure–function studies of the hammerhead [5–7], hairpin [8–10], *glmS* [11–13], hepatitis delta virus (HDV) [14–16] and Varkud satellite (VS) [4,17,18] ribozymes. Structural studies of these ribozymes in their pre-catalytic, and in some cases in vanadate transition state mimic conformations, have provided insights into their overall architecture, the topology of their catalytic active site organization, and the role of nearby nucleobases and hydrated divalent cations in facilitating general acid-base and electrostatic-mediated catalysis [19,20••,21–25].

A working hypothesis regarding natural self-cleaving ribozymes is that they utilize a network of defined hydrogen bonds, ionic and hydrophobic interactions to generate catalytic pockets, which capitalize on steric constraints to generate in-line cleavage alignments and general acid-base chemistry to catalyze site-specific cleavage of the phosphodiester backbone. There is general agreement that there are four factors that can contribute to RNA phosphodiester cleavage involving targeting by the 2′-OH group of the adjacent P-O5′ bond at the scissile phosphate associated with a pentacoordinated phosphorane transition state intermediate (Figure 1a) [19]. These include contributions from in-line alignment of the 2′-O atom and the to-be-cleaved P-O5′ bond (α factor); those associated with electrostatic compensation resulting from the enhanced negative charge on the non-bridging scissile phosphate oxygens in the transition state (β factor); those of general base in activating the 2′-OH for nucleophilic attack on the scissile phosphate (γ factor); and those of general acid in donating a proton to the developing negative charge on the O-5′ leaving group (δ factor). For a given ribozyme, revealing which combination of factors contribute and predominate, remains a challenge,

Figure 1

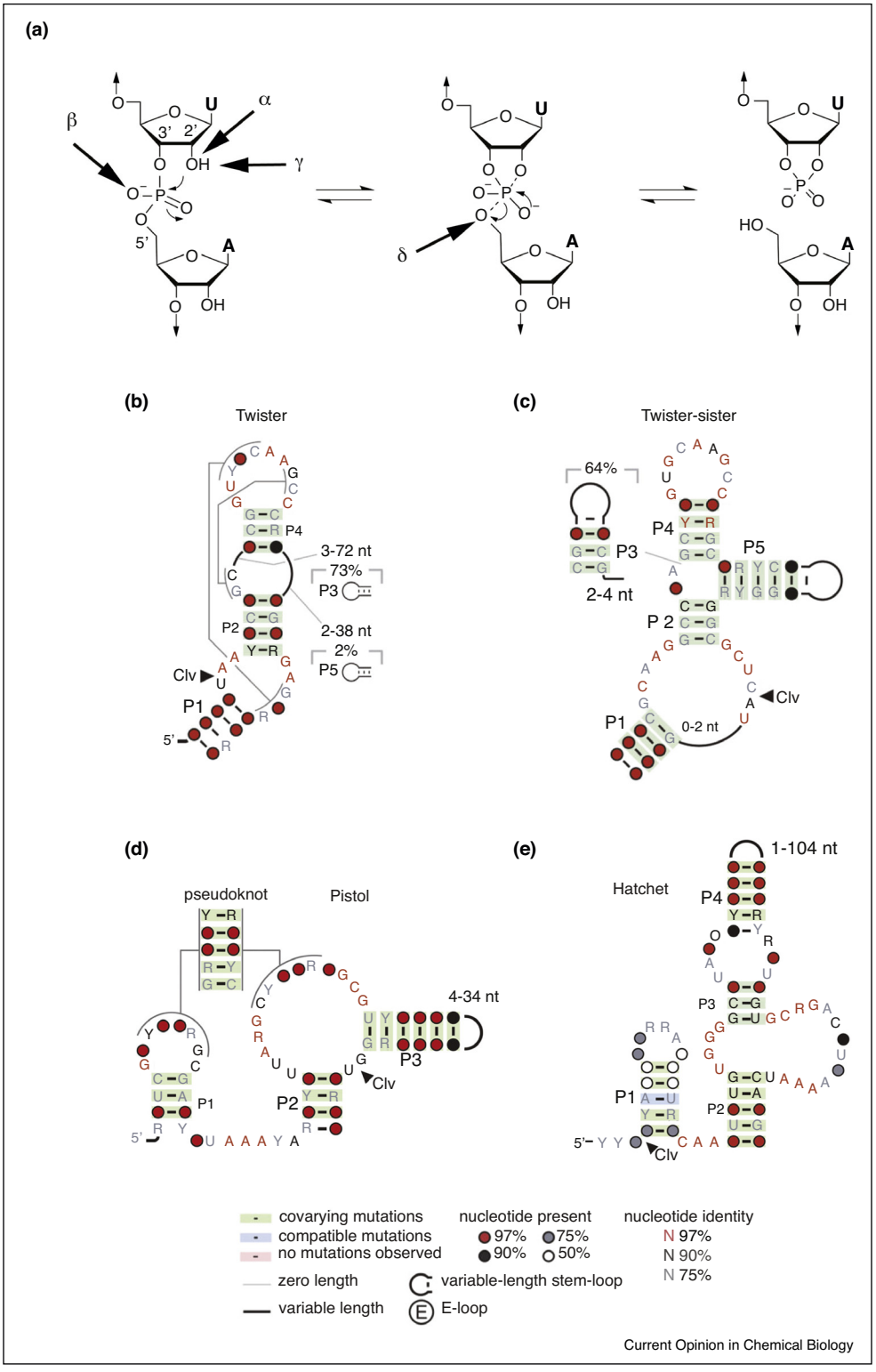

Catalytic strategies for cleavage of the phosphodiester backbone by self-cleaving ribozymes, as well as consensus sequences and secondary structures of newly-identified self-cleaving twister, twister–sister, pistol and hatchet ribozymes. **(a)** Four factors that can contribute to catalysis during internal phosphodiester transfer reaction. α factor: in-line alignment of the 2′-O, phosphorus and O-5′ at the scissile phosphate; β factor: neutralization of the developing negative charge on the nonbridging phosphate oxygen; γ factor: general base-mediated deprotonation of the 2′-O; δ factor: general acid-based neutralization of the developing negative charge in the O-5′ position. (Adopted from [19]). **(b–e)** Consensus sequence

as does whether phosphodiester bond cleavage could occur via a concerted or a stepwise manner.

The recent discovery of four natural self-cleaving ribozymes named twister, twister–sister, pistol and hatchet (Figure 1b–e) from a bioinformatic genomic analysis [1••,26•] provide a subset of new ribozymes that can be comparatively investigated from a structural perspective, with their subsequent molecularly-defined active sites probed using structural-chemical activity relationships to understand their mechanism(s) of action. Thus, once structures are available, the catalytic mechanism can be probed by site-specific substitutions and modifications of bases and phosphates lining the catalytic pocket and through monitoring of shifted pK_a's of bases with potential involvement in the cleavage mechanism. Such studies could lead eventually to engineered small-size ribozymes with tunable cleavage specificities and activities for applications in biotechnology and biomedicine.

Nevertheless, many mechanistic questions related to ribozyme catalysis remain unanswered: Are catalytic pockets restricted to multi-helical junctions and/or pseudoknots and what factors define the relative alignments of residues essential for site-specific catalysis? Do invariant residues form tertiary contacts, and if so, how do functional group proximity and orientation impact on general acid-base catalysis and contribute to transition state stabilization? How critical are unstacked splayed-out orientations of the nucleotides flanking the scissile phosphate and the relative contributions to their stabilization by a combination of cross-strand base pairing and unconventional stacking interactions? Also, a range of potential nucleophiles have been proposed as general bases for activation of the sugar 2′-OH group, while both guanines and adenines have been proposed as general acids for protonation of the O-5′ leaving group, with little consensus between ribozyme systems. What is the role of hydrated Mg^{2+} cations in stabilizing the developing negative charge in the transition state? Given that each ribozyme has a unique overall architecture and active site orientation, do they use distinct or common principles to perform the same internal transesterification reaction.

The current review, which builds on a previous comprehensive review on hammerhead, hairpin, HDV, VS and *glmS* self-cleaving ribozymes [20••], will begin by focusing on recent structural research on the pre-catalytic and transition state mimic conformations of the Rzb hammerhead ribozyme and outline how these studies have advanced our knowledge of the catalytic mechanism underlying self-cleavage by this previously well-studied family of ribozymes. Next, the review will focus on recent structural and mutational research on the pre-catalytic state of the pistol ribozyme, for which a consensus is emerging as to its catalytic mechanism. This will be followed by related studies on the twister and twister–sister ribozymes, for which there are conflicting structural perspectives as to the active site alignments and catalytic mechanisms, based on pre-catalytic conformations of both ribozymes.

Hammerhead ribozyme

The hammerhead ribozyme is amongst the most intensely studied self-cleaving ribozymes from both a structural and functional perspective. Early structural studies on truncated hammerhead ribozymes [27,28] yielded results that contradicted mechanistic insights from functional studies [29]. This conundrum was only resolved following structure determination of a longer hammerhead ribozyme construct that included flanking segments involved in tertiary contacts distant from the active site required for priming ribozyme catalysis, resulting in a thousand-fold catalytic enhancement [6]. The secondary and tertiary folds, together with the three-dimensional structure of the hammerhead ribozyme, are shown in Supplementary Figure 1a–c, respectively. The alignment in the catalytic pocket is shown in Supplementary Figure 1d, with splaying apart at the C17-C1.1 cleavage step. Notably, nucleobase G12 is directed towards the 2′-O of C17, while the 2′-OH of G8 is directed towards the O-5′ of C1.1 [6].

These studies have been recently expanded to the Rzb hammerhead ribozyme (Figure 2a) to elucidate the potential role of conformational changes and divalent metal ions on proceeding from pre-catalytic to transition state conformations to ribozyme-mediated catalysis [30••,31•]. The three-dimensional topology and structure of this ribozyme are shown in Figure 2b and c. The major advance over earlier studies involved identification of conformational rearrangements in the catalytic pocket prior to the cleavage reaction, with positioning of a pair of divalent cations (either Mg^{2+} or Mn^{2+}) facilitating the process. One divalent cation (labeled M2) is directly coordinated to the O6 of G12, with the potential to lower its pK_a, thereby facilitating its likely role as a general base, a conclusion supported by the results of molecular dynamics simulations [32]. A second divalent cation (labeled M1) bridges the N7 of G10.1 and the scissile phosphate, raising the possibility of hydrated divalent cation participation in the cleavage process (Figure 2d) [31•]. Further studies on a vanadate transition state mimic of the Rzb hammerhead ribozyme resulted in movement of G12 closer to the 2′-O of C17, as well as repositioning of G10.1, such that M1 is now positioned closer to the

(Figure 1 Legend Continued) and secondary structures of newly-identified self-cleaving twister (panel b), twister–sister (panel c), pistol (panel d) and hatchet (panel e) ribozymes.
Adopted from [26•,51].

Figure 2

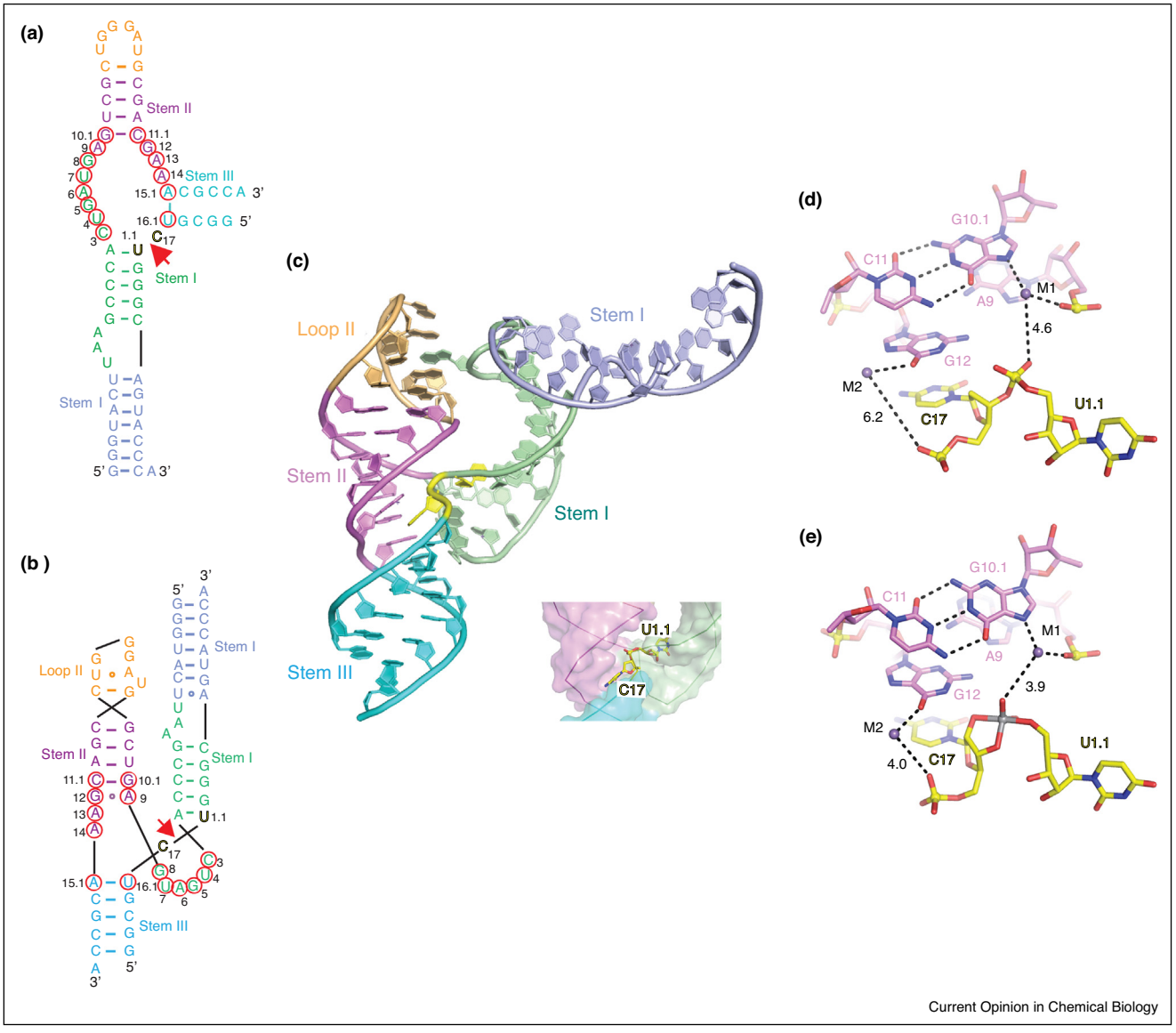

Secondary, tertiary and three-dimensional structures of Rzb hammerhead ribozyme [30••,31•], together with details of residues and divalent cation positioning centered about the cleavage step. **(a–e)** Schematics of the secondary (panel a) and tertiary (panel b) folds and a ribbon three-dimensional structure (panel c), as well as details of residue positioning centered about the cleavage site (panel d) of the pre-catalytic state of the Rzb hammerhead ribozyme (PDB: 5DI2). The Mn^{2+} (M1) to non-bridging scissile phosphate oxygen is 4.6 Å in panel d. Details of residue and divalent cation positioning centered about the cleavage site (panel e) of the transition state vanadate mimic of the Rzb hammerhead ribozyme (PDB: 5EAQ). The Mn^{2+} (M1) to non-bridging scissile phosphate oxygen is 3.9 Å in panel e.

scissile phosphate, thereby positioning its divalent cation-bound water opposite the oxygens of the scissile phosphate, with a potential role for this water in catalysis (Figure 2e) [30••]. These pioneering studies [30••,31•] definitively established a key role for a pair of active site divalent cations (Mg^{2+} or Mn^{2+}) in cleavage chemistry.

Pistol ribozyme

The small self-cleaving pistol ribozyme is composed of three stems, a hairpin loop and an internal bubble, as shown schematically in Figure 1d [1••,33]. Highly conserved nucleotides are primarily located in the internal bubble and the linker segment (containing a AAA trinucleotide), while segments of the hairpin loop and internal bubble are predicted to be involved in a 6-nt pseudoknot formation. Cleavage occurs at a modestly conserved G-U dinucleotide junctional step whose two-nucleotide length is strictly conserved. RNA cleavage was shown to be dependent on Mg^{2+} and the cleavage rate increased with increasing pH. Studies using phosphorothiolate substitution at the

cleavage site suggest that the pistol ribozyme exploits a contact between one of two non-bridging phosphate oxygens and the ribozyme to facilitate catalysis. Metal ion-dependent studies have been interpreted to conclude that the pistol ribozyme does not require inner-sphere coordination of divalent cation for catalysis. RNA strand scission occurs with a rate constant of 10 min^{-1} under physiological pH and Mg^{2+} conditions [33].

Structural studies have focused on a two-stranded *env25* pistol ribozyme construct (Figure 3a) containing dG at the G-U cleavage site with the tertiary fold and three-dimensional structure shown in Figure 3b and c, respectively [34••]. This pre-catalytic conformation of the pistol ribozyme adopts a compact tertiary architecture stabilized by an embedded pseudoknot fold (Figure 3a–c). The G53-U54 cleavage site adopts a splayed-apart conformation (Figure 3c, insert), while the conserved AAA segment is positioned through A-minor base triple formation in the minor groove of stem P1 (Figure 3c). Both G53 and U54 are anchored through intercalation between bases (Figure 3d), such that the modeled 2′-O of G is positioned for in-line attack on the adjacent to-be-cleaved P-O5′ bond (Figure 3e). Highly conserved residues G40 (N1 position, red arrow) and A32 (N3 and 2′-OH positions, black arrows) are aligned (Figure 3e) to potentially act as general base and general acid respectively, to accelerate the cleavage chemistry, with their roles supported from cleavage assays on the A mutant of G40, as well as C, dA and c^3dA mutants of A32 [34••]. NMR studies on a site-specifically ^{13}C-C2-labeled A32 pistol ribozyme yielded a shifted pK_a of 4.7 for A32 compared to a pK_a of 3.7 for adenine at the oligomer level. A hydrated Mg^{2+} is also positioned opposite the scissile phosphate, with a Mg^{2+} to non-bridging oxygen of the scissile phosphate distance of 4.0 Å (Figure 3e). Further, mutation of the conserved AAA segment to UUU, impacted on cleavage activity. A 2-aminopurine-incorporated fluorescence-based approach was used to measure a cleavage rate for the pistol ribozyme in 10 mM Mg^{2+} of k_{obs} = 0.88 min^{-1} at 15 °C [34••]. Given that both G53 and U54 are held in place in an in-line alignment through intercalation between bases in the pre-catalytic conformation (Figure 3d), it is unlikely that they will undergo substantial conformational changes in the transition state conformation. The same overall fold and active site alignment was subsequently validated for the structure of the pre-catalytic conformation of a related pistol ribozyme [35•], except that the putative general acid A32 in [34••] was replaced by a G in [35•]. It is therefore likely that N3 of A32 and G32 may play comparable roles in catalysis, although an experimental validation via 3-deaza ribonucleoside (c3A and c3G) substitutions is still pending.

Furthermore, it appears that the use of guanine as a general base and adenine as a general acid, are features common to pistol [34••,35•], hairpin [8,9] and VS [17] ribozymes, with the distinction that for the pistol ribozyme it is the purine N3 and/or ribose 2′-OH positions, while in the hairpin and VS ribozymes it is the adenine N1 position, that is involved in general acid catalysis.

Twister ribozyme

The self-cleaving twister ribozyme exhibits the general secondary structure shown in Figure 1b [1••,26•]. This ribozyme consists of three stems conjoined by internal bubbles and terminal loops, with its catalytic activity predicted from phylogenetic analysis to be dependent on formation of two pseudoknots (Figure 1b). Efficient substrate processing occurred at a U-A step, with cleavage rate constants strongly dependent on Mg^{2+} concentration. In addition, cleavage rates exhibited a bell-shaped pH dependence, plateauing at a pH value of 6.5 [26•].

To date, several x-ray structures have been reported of the twister ribozyme [36•,37,38••,39••] that define the same global fold but differ in details of residue orientation within the catalytic pocket, as well as the role of divalent cations. One study focused on a two-stranded *env22* twister ribozyme construct (Figure 4a) containing dU5 at the U5-A6 cleavage site, with the tertiary fold schematic and three-dimensional structure shown in Figure 4b and c, respectively [39••]. This pre-catalytic conformation of the twister ribozyme adopts a compact tertiary architecture stabilized by co-linear stacking of helical stems and a pair of long-range pseudoknots interactions (Figure 4a–c), with a splayed apart U5-A6 step positioned in the center of the fold (insert, Figure 4c). Ten strongly conserved nucleotides distributed between internal bubble L1 and terminal stem-loop SL4 are brought into close proximity, with the active site center composed of pseudoknot T1 and U5-A6 step-containing junction J1-2 (Figure 4b and c).

The highly conserved A6 base adopts a *syn* glycosidic alignment stabilized by stacking interactions, while U5, which is not conserved, appears to adopt a flexible alignment. In addition, the N1H of G48 forms a strong hydrogen bond to the non-bridging *pro-R_P* phosphate oxygen (Figure 4d), while a hydrated Mg^{2+} cation (green ball) is directly coordinated to the non-bridging *pro-S_P* phosphate oxygen at the U5-A6 step (Figure 4d), with near in-line arrangement at the scissile phosphate. From a comparative perspective, direct coordination of a hydrated Mg^{2+} cation to a non-bridging phosphate oxygen of the scissile phosphate has been previously reported for the pre-catalytic conformation of the HDV ribozyme [40,41].

Site-specific modifications imply that A6 and G48, but not U5, play critical roles in the self-cleavage catalytic mechanism of the twister ribozyme [39••]. Further, no cleavage was observed for either 2-aminopurine or 1,3-dideaza adenine (c^1c^3A) substitutions at position A6 of the twister

Figure 3

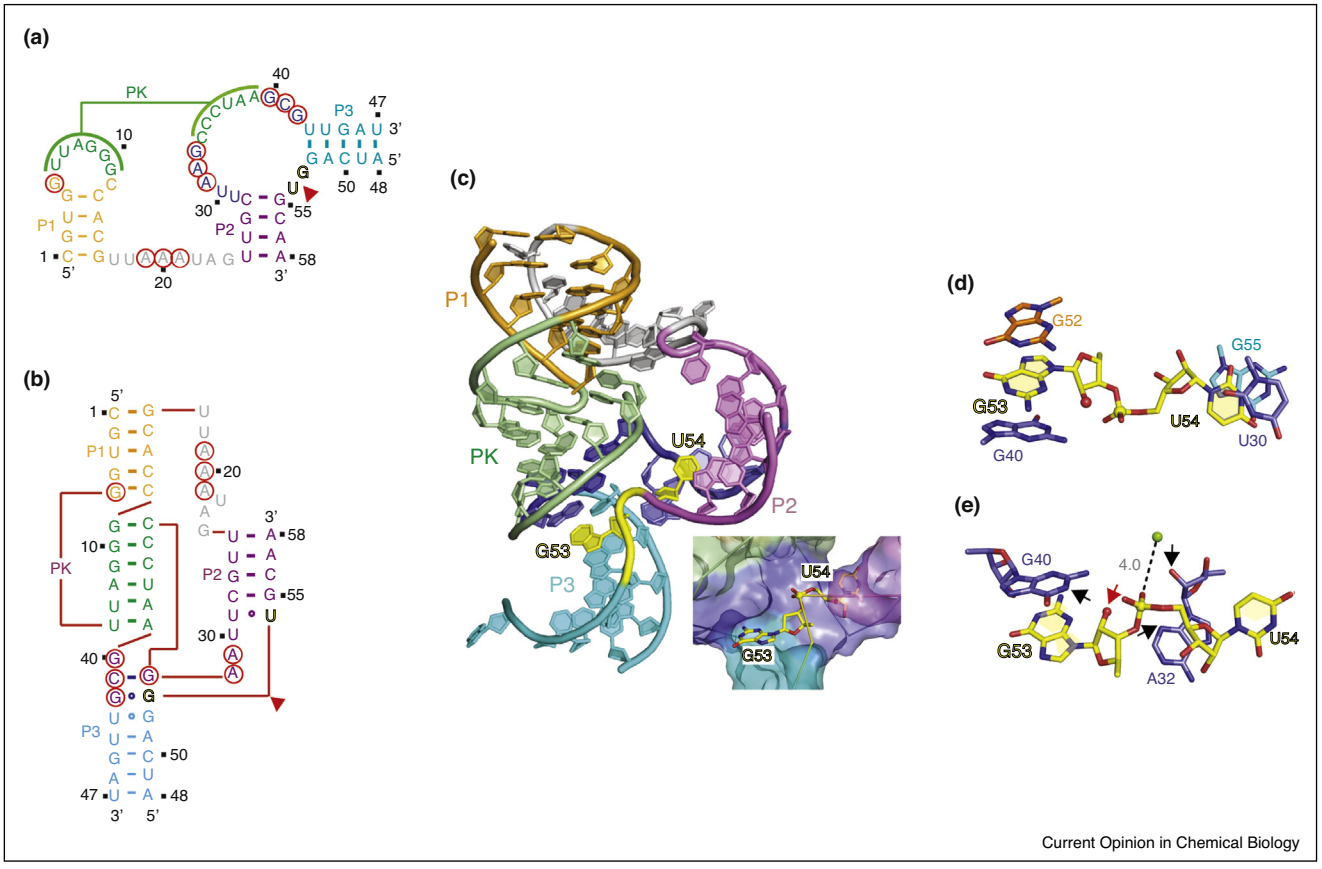

Secondary, tertiary and three-dimensional structures of the *env25* pistol ribozyme [34••] together with details of residues and divalent cation positioning centered about the cleavage step. **(a–e)** Schematics of the secondary (panel a) and tertiary (panel b) folds together with a ribbon three-dimensional structure (panel c), as well as details of residue positioning centered about the cleavage site (panels d and e) of the pre-catalytic state of the pistol ribozyme (PDB: 5K7C). Highly-conserved residues are designated by red circles and the cleavage site by a red arrow in panels a and b. The splayed-apart G53-U54 cleavage step is colored in yellow and is highlighted in the box attached to panel c. Panel d emphasizes the anchoring of G53 and U54 through intercalation. Panel e emphasizes details of residues and hydrated divalent cation positioning centered about the cleavage step. The 2′-O of G53 is labeled by a red arrow, while the N3 and 2′-OH of A32 are labeled by black arrows in panel e. The Mg^{2+} to non-bridging scissile phosphate oxygen distance is 4.0 Å in panel e.

ribozyme, emphasizing the importance to catalysis of the 6-amino and N1/N3 positions of A6, consistent with a shifted pK_a of 5.1 for this residue [36•]. No definitive conclusion could be reached on the contribution to catalysis of the directly coordinated Mg^{2+} cation, given that only a modest 2-fold enhancement was observed on thio substitution rescue at the scissile phosphate on replacement by Mn^{2+} and Cd^{2+} ions [36•]. A molecular dynamics computational study starting from the structure of the *env22* twister ribozyme has predicted a role for monovalent Na^{+} cation positioned next to the O-5′ leaving group atom to cleavage chemistry [42]. Fluorescence-based studies using a 2-aminopurine substituted marker yielded a cleavage rate of $k_{obs} = 2.4 \pm 0.3\ min^{-1}$ for the twister ribozyme [39••].

Surprisingly, stem P1 is stabilized by only two (of four potential) Watson-Crick base pairs in the structure of the *env22* twister ribozyme, with disrupted bases U1 and U4 (Figure 4b) instead participating through fold back in formation of stacked base triples [39••,43]. Indeed, wild-type cleavage activity was observed even when the phylogenetically conserved stem P1 was deleted, and accompanied by site-specific cleavage of a single nucleoside [36•,44]. A recent single-molecule FRET study on twister ribozyme folding rationalizes this behavior by revealing that the active site-embracing pseudoknot fold is preserved in the shortened ribozyme and in the cleaved 3′-product RNA that both lack P1 [45•].

A second group has reported on the crystal structure of the *Oryza sativa* twister ribozyme composed of a secondary structure shown in Figure 4e, with the three-dimensional structure shown in Figure 4f [38••,46•]. This construct differs from the *env22* twister ribozyme in that it lacks stem P3, and in addition, contains a fully-paired stem P1

Figure 4

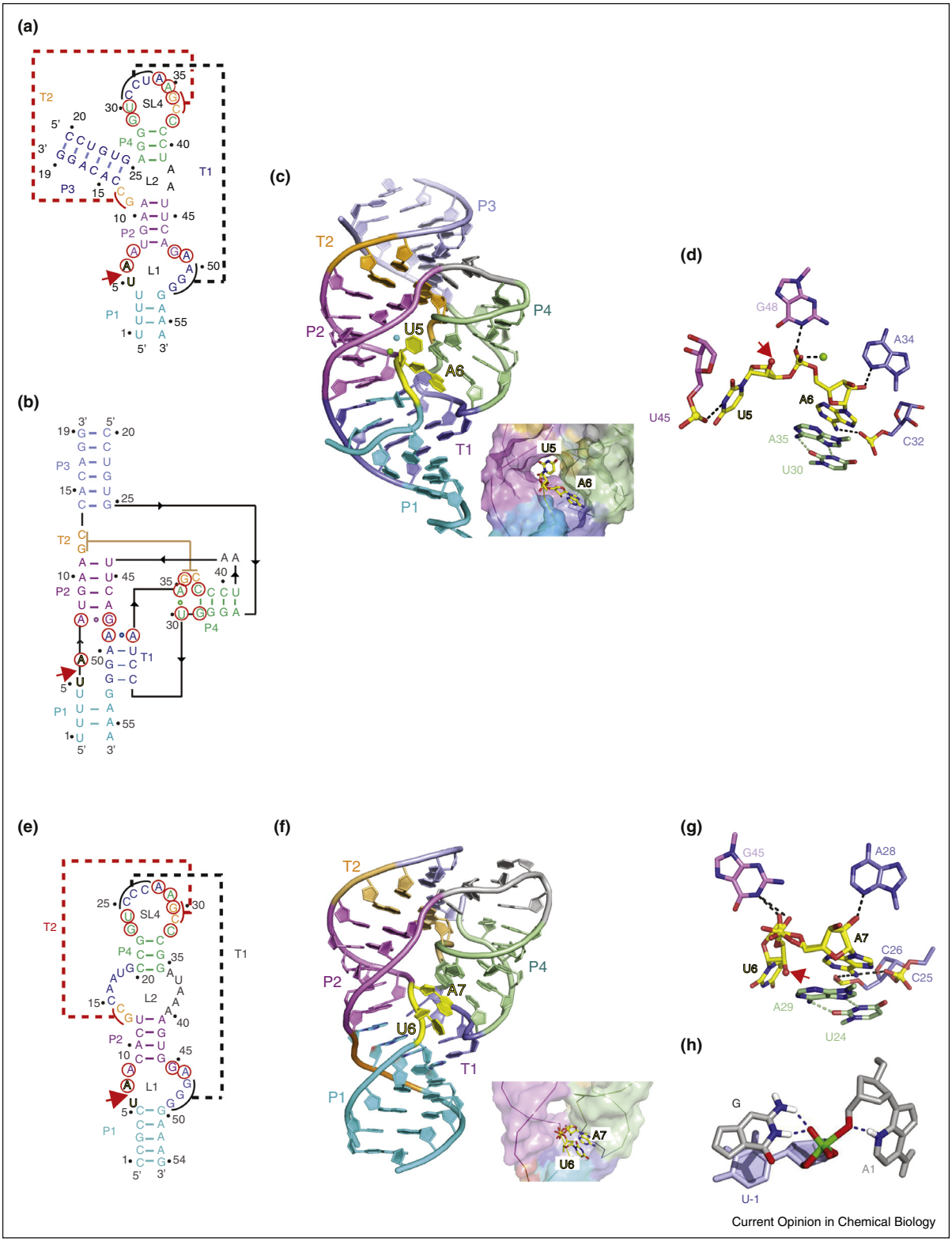

Secondary, tertiary and three-dimensional structures of the *env22* [39••] and *O. sativa* [38••] twister ribozymes together with details of residues and divalent cation positioning centered about the cleavage step. **(a–d)** Schematics of the secondary (panel a) and tertiary (panel b) folds, together with a ribbon three-dimensional structure (panel c), as well as details of residue positioning centered about the cleavage site (panel d) of the pre-catalytic state of the *env22* twister ribozyme (PDB: 4RGE). Highly-conserved residues are designated by red circles and the cleavage site by a red

(Figure 4e). At the global level, the pre-catalytic conformations of the *env22* (Figure 4c) and *O. sativa* (Figure 4f) twister ribozymes adopt similar folds stabilized by the same dual pseudoknot and non-canonical pairing interactions, as well as an anchored *syn* A base at the cleavage site. In addition, the same invariant guanine (G48 in *env22* and G45 in *O. sativa* ribozymes) and the same invariant adenine at the U-A cleavage step (A6 in *env22* and A7 in *O. sativa* ribozymes) are proposed to be involved in acid-base catalysis (Figure 4d and g). Nevertheless, there are important differences centered about the scissile U-A step between the structures of the two twister ribozymes. Thus, the *O. sativa* twister ribozyme adopts an off-line alignment with no hydrated Mg^{2+} cation observed in the vicinity of the scissile phosphate oxygens (Figure 4g). Given that the U at the U-A cleavage step was involved in packing interactions in the crystal lattice in the pre-catalytic structure of the *O. sativa* twister ribozyme, it was proposed that the off-line conundrum could be potentially resolved through incorporation of a sizeable conformational change in the U base to position it for in-line attack [38••]. Molecular dynamics studies starting from the off-line structure of the *O. sativa* ribozyme have postulated a transition state alignment where the U base adopts an in-line alignment stabilized by stacking with G45, whose N1H and NH_2-2 protons are hydrogen bonded to the same non-bridging phosphate oxygen, while the N3 of A is positioned to donate a proton to the P-O5′ oxygen (Figure 4h) [47•]. Further experimentation using base analogs will be required to test this proposed computational model for the transition state of the twister ribozyme in solution.

The observed differences between the active site alignments at the U-A cleavage step between the pre-catalytic conformations of the *env22* and *O. sativa* twister ribozymes (Figure 4d and g) remain to be resolved [19,44], especially the contribution of a hydrated Mg^{2+} cation to cleavage chemistry. In the most optimistic scenario, these differences may reflect the requirement of conformational flexibility of the U base for the functioning of the twister ribozyme, with the distinct pre-catalytic conformations adopted by the *env22* and *O. sativa* twister ribozymes perhaps representing snapshots of relevant alignments on the pathway to cleavage. Clearly, there is a critical need to go beyond pre-catalytic conformations and instead focus on determining the structure of a transition state vanadate mimic conformation of the twister ribozyme, as the most direct approach towards resolving the existing conundrum.

Twister–sister ribozyme

The self-cleaving twister–sister ribozyme exhibits either a three-way or four-way junctional fold conjoined by internal and terminal loops (these loops containing conserved residues are similar to those in the twister ribozyme) as shown in Figure 1c [1••]. Efficient substrate processing occurs at a C-A step, on the opposite face of an internal loop (Figure 1c) when compared to the related twister ribozyme (Figure 1b). Furthermore, like twister, twister–sister ribozyme displays an approx. 10-fold increase in cleavage activity with each increase in pH unit, reaching a plateau near pH 7 [1••]. It was therefore speculated that the simplest explanation for this pH-activity profile is that the ribozyme shifts the pK_a of the 2′-OH of cytidine at the scissile phosphate to approx. 7, supporting its deprotonation for efficient nucleophilic attack [1••]. Nevertheless, the structural basis for the putative pK_a shift has remained unclear.

One group has now solved the structure of a two-stranded four-way junctional fold containing dC-A at the cleavage step of the twister–sister ribozyme (Figure 5a), with the tertiary fold schematic and three-dimensional structure shown in Figure 5b and c, respectively [48••]. Notably, SL4 projecting from continuous helix P5-P4 is positioned in the minor groove of the partially zippered-up L1 loop segment associated with the continuous P1-P2-P3 helix (Figure 5b and c). Several looped-out bases (A7, G35 and U36) form long-range contacts (labeled T1 and T2) in the tertiary fold of the twister–sister ribozyme (Figure 5a–c).

Bases C62 and A63 at the cleavage site are splayed apart, with flexible C62 directed outwards and A63 directed inwards and anchored in place within the ribozyme fold (Figure 5d). Notably, the N1H of G5 and an inner sphere water of hydrated Mg^{2+} cation (labeled M1) form hydrogen bonds to the non-bridging phosphate oxygens, thereby anchoring the scissile phosphate in place. In addition, a hydrated Mg^{2+} (labeled M2) is positioned such that an inner sphere water is within hydrogen bond distance of the modeled 2-O′ of C62 at the cleavage step. Mutations of G5 and inwardly-oriented and anchored A63

(Figure 4 Legend Continued) arrow in panels a and b. The splayed-apart U5-A6 cleavage step is colored in yellow and is highlighted in the box attached to panel c. The 2′-O of U5 is labeled by a red arrow, with the N1 of G48 and a Mg^{2+} cation directly coordinated to different non-bridging phosphate oxygens of the scissile phosphate in panel d. Base U5 is flexible while base A6 is anchored by stacking on a base pair in panel d. **(e–h)** Schematic of the secondary structure (panel e), together with a ribbon three-dimensional structure (panel f), as well as details of residue positioning centered about the cleavage site (panel g) of the pre-catalytic state of the *O. sativa* twister ribozyme (PDB: 4QJI). The partially-stacked U6-A7 cleavage step is colored in yellow and is highlighted in the box attached to panel f. The 2′-O of U5 is labeled by a red arrow, with the N1 of G45 directed towards the 2′-O of U6 in panel g. Two alternate alignments of the scissile phosphate are shown in panel g. Base U6 is flexible while *syn* A7 is anchored by stacking on a base pair in panel g. (h) Alignment at the cleavage step deduced from a molecular dynamics simulation starting from the crystal structure of the *O. sativa* twister ribozyme [47•]. The residues at the cleavage step are labeled U-1 and A1 corresponding to U6 and A7 in the crystal structure of the *O. sativa* twister ribozyme.

Figure 5

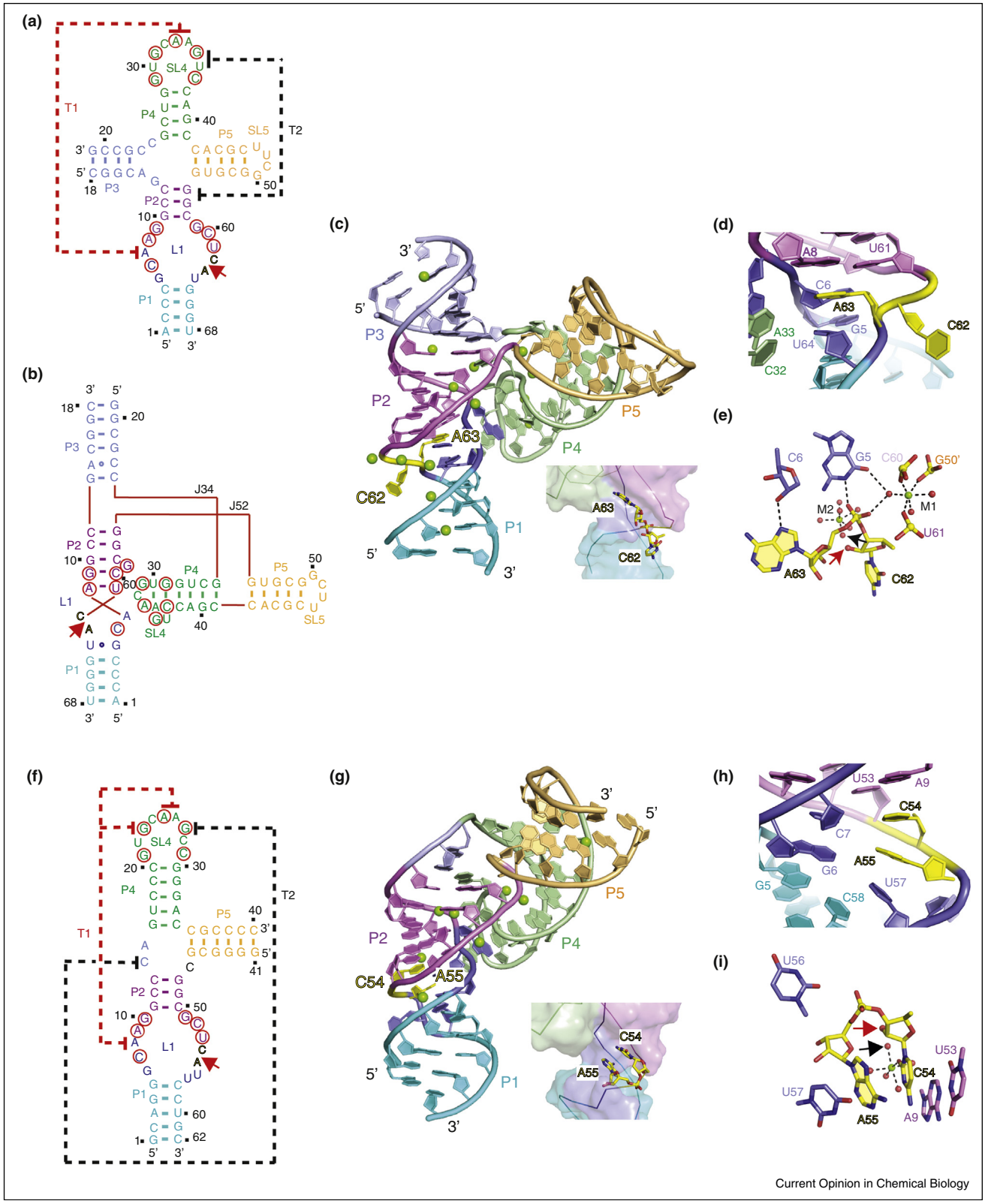

Secondary, tertiary and three-dimensional structures of four-way [48••] and three-way [49••] junctional twister–sister ribozymes together with details of residues and divalent cation positioning centered about the cleavage step. **(a–e)** Schematics of the secondary (panel a) and tertiary (panel b) folds, together with a ribbon three-dimensional structure (panel c), as well as details of residue positioning centered about the cleavage

result in complete loss in cleavage activity, while mutation of flexible and outwardly-oriented C62 has no impact on activity. Replacement of the phosphate linking C60 and U61, which is involved in coordination to hydrated metal M1 (Figure 5c), by methylphosphonate, was slightly impaired in cleavage activity.

A second group has reported on the crystal structure of a two-stranded three-way junctional fold of the twister–sister ribozyme (lacking stem P3) composed of a secondary structure shown in Figure 5f, with the three-dimensional structure shown in Figure 5g [49••]. The cleavage rate of this ribozyme showed a log-linear correlation with divalent metal ion pK_a. A comparative analysis of the global architectures showed that the long-range interactions that define the tertiary fold of the twister–sister ribozyme show both similarities (long-rang contact labeled T1) and differences (long-range contact labeled T2) between three-way [49••] and four-way [48••] junctional structures (Figure 5f and a). Both pre-catalytic states structures of the twister–sister ribozyme exhibit off-line alignments, with the modeled 2′-OH of C at the cleavage site within hydrogen bonding distance of an inner sphere water of a hydrated Mg^{2+} cation (Figure 5e and i). By contrast, the C and A are stacked, with C adopting an anchored and A a flexible alignment in the three-way junctional structure (Figure 5h and i) [49••], while the C-A step is splayed apart, with C adopting a flexible and A an anchored alignment in the four-way junctional structure (Figure 5d and e) [48••]. Further, neither a G nor a hydrated Mg^{2+} is coordinated to the oxygens of the scissile phosphate in the three-way junctional structure (Figure 5h and i) [49••], as it is in the four-way junctional structure (Figure 5d and e) [48••]. These pronounced differences within the catalytic pocket of the pre-catalytic states of these two reported structures reinforce the need for structure determination of transition state vanadate mimics of the twister–sister ribozyme to clarify an otherwise conflicting situation from a structural perspective.

Hatchet ribozyme

The sequence of the hatchet ribozyme identified in the Breaker laboratory is outlined in Figure 1e [1••,50]. There are as yet no reported structures of pre-catalytic or transition state analogs of the hatchet ribozyme to complement available biochemical data [50] on this self-cleaving ribozyme. The hatchet ribozyme sequence contains 13 highly conserved residues interspersed amongst bulge elements linking stem segments (Figure 1e). RNA strand scission in the hatchet ribozyme exhibits an essential requirement for divalent Mg^{2+} cations, with a measured maximum cleavage rate k_{obs} of approx. 4 min^{-1} that plateaus on increasing the pH to 7.5. Rate measurements on phosphorothiolate analogs positioned at the cleavage step are suggestive of a critical contact between a moiety within the active site of the ribozyme and the non-bridging phosphate oxygen at the cleavage step [50]. In addition, the pH reactivity profile suggests that the 2′-OH of the attacking nucleophile is activated by a functional group that has a pK_a in the pH 7 range [50].

The positioning of the cleavage site at the 5′-end separated from the secondary structural elements in the hatchet ribozyme is reminiscent of the *glmS* ribozyme [11,12], and it will be interesting to elucidate what novel folding topology of the hatchet ribozyme will position the broadly distributed conserved residues proximal to the cleavage site. Of particular interest will be to compare structural-chemical-activity relationships between the hatchet and *glmS* ribozymes, keeping in mind that the *glmS* ribozyme is dependent on cofactor GlcN6P for its activity. Further, since structures are available for substrate, transition and cleaved states (the cleavage pocket is preformed) of the *glmS* ribozyme [11,12], a comparison with their counterparts in the hatchet ribozyme, once available, would be illuminative of similarities and differences between these two ribozymes.

Evolution of self-cleaving ribozymes

According to the RNA world hypothesis, catalytic RNA played a crucial role in the early origin of life [52–54]. RNA evolution in the laboratory (*in vitro* selection) thereby gave an idea on how broad the diversity of chemical reactions is that can be catalyzed by RNA. These include nucleotide synthesis, RNA polymerization, aminoacylation of transfer RNA, and peptide bond formation [55–58]. In contemporary biology, most RNA catalysts such as ribosomes, splicosomes, and ribonucleases P have evolved from their ancient RNA ancestors to become decorated with protein components to ensure their functions in modern cells [59,60]. Small

(Figure 5 Legend Continued) site (panels d and e) of the pre-catalytic state of the four-way junctional twister–sister ribozyme (PDB: 5Y85). Highly-conserved residues are designated by red circles and the cleavage site by a red arrow in panels a and b. The splayed-apart C62-A63 cleavage step is colored in yellow and is highlighted in the box attached to panel c. The splayed apart alignment of the C62-A63 step involving looped out C62 and stacked A63 is highlighted in panel d. The 2′-O of C62 is labeled by a red arrow, with the N1 of G5 and an inner sphere water of hydrated Mg^{2+} cation M1 hydrogen bonded to different non-bridging phosphate oxygens of the scissile phosphate in panel e. In addition, an inner sphere water of hydrated Mg^{2+} cation M2 labeled by a black arrow can form a hydrogen bonded to the 2′-O of C62 in panel e. **(f–i)** Schematic of the secondary structure (panel f), together with a ribbon representation of the three-dimensional structure (panel g), as well as details of residue positioning centered about the cleavage site (panels h and i) of the pre-catalytic state of the three-way junctional twister–sister ribozyme (PDB: 5T5A). The fully-stacked C54-A55 cleavage step is colored in yellow and is highlighted in the box attached to panel g. The stacked alignment of the C54-A55 step is highlighted in panel h. The 2′-O of C54 is labeled by a red arrow, while an inner sphere water of a hydrated Mg^{2+} cation labeled by a black arrow is positioned to form a hydrogen bonded to the 2′-O of C54 in panel i.

self-cleaving ribozymes therefore appear to be the only extant RNA catalysts that still act without the assistance of proteins. They catalyze phosphordiester cleavage in different mechanistic flavors, based on more than ten distinct classes known today [61]. It is yet unknown whether these classes have developed in independent manner or whether some of them have related evolutionary pathways, for example, by escaping the parent ribozyme fold through defined mutations [62,63]. Further dedicated investigations and well-designed experiments will be needed to shed light on ribozyme evolution not only in a presumed ancient RNA world but also in modern organisms.

Conclusions

Our current understanding of catalytic mechanisms adopted by small self-cleaving ribozymes represents a work in progress [19]. Of the ribozymes discussed in this review, the most detailed structural information involving both pre-catalytic and transition state vanadate mimics is available for the Rzb hammerhead ribozyme, highlighting the role of conformational changes and divalent cations to ribozyme-mediated catalysis (Figure 2) [30••,31•]. There is also a common consensus on a general acid-base catalytic mechanism for the pistol ribozyme, where both bases at the cleavage step are anchored through intercalation in the pre-catalytic conformation, with nearby guanine (opposite 2′-O) and adenine or guanine (opposite O-5′) positioned to function in general acid-base catalysis (Figure 3) [34••,35•].

By contrast, there are significant differences in pre-catalytic conformations of the active site for different constructs studied by two groups of both the twister (Figure 4) [38••,39••], and twister–sister (Figure 5) [48••,49••] ribozymes. Thus, while one group observed splayed apart conformations at the cleavage site, together with a guanine hydrogen bonded to and a hydrated Mg^{2+} cations coordinated to the scissile phosphates for both ribozymes [39••,48••], another group observed partial/fully-stacked conformations at the cleavage site, guanines directed to the 2′-O (for twister but not twister–sister) and the absence of hydrated Mg^{2+} cations coordinated to the scissile phosphate for both ribozymes [38••,49••]. While one group favors a common catalytic mechanism involving a combination of general-acid base and hydrated divalent cation involvement in catalysis for both twister and twister–sister ribozymes [39••,48••], similar to what has been proposed for the HDV ribozyme [41], the other group favors a general acid-base mechanism for the twister ribozyme [38••] and postulates that twister–sister primarily functions as a metalloenzyme [49••]. The resulting mechanistic disagreements [19] will require resolution in the future, with one promising approach involving undertaking structural studies of transition state vanadate mimics of both twister and twister–sister ribozymes to resolve the ongoing conundrum.

Updates

Several papers on self-cleaving ribozymes have appeared between submission of the review and its publication. We briefly describe the pertinent advances below.

Pistol ribozyme

The role of conserved A32 (see labeling in Figure 3a and e), that lines the catalytic pocket in the crystal structure of the pistol ribozyme reported in Figure 3e, in general acid catalysis, has been probed from studies of analogs A32c^{1}A, A32c^{3}A, A32Pu, A32A(2′-OCH_3) and A32A(2′-NH_2) (Neuner *et al.*, unpublished data). The authors conclude that A32 more likely plays a structural rather than a catalytic role in the cleavage chemistry of the pistol ribozyme.

Twister ribozyme

Both bulk FRET and single-molecule FRET together with activity assays have been applied to understand the role of divalent cations in promoting folding and self-cleavage of the *O. sativa* twister ribozyme. The authors conclude that divalent cations induce transient folding and activation of the twister ribozyme, with 25-fold less Mg^{2+} required for self-cleavage compared to folding of the ribozyme [64•]. Notably, Co^{2+}, Ni^{2+} and Zn^{2+} were found to be more efficient in cleavage relative to Mg^{2+}.

Twister–sister ribozyme

Molecular dynamics and molecular solvation theory have been applied in attempts to compute the transition state conformation of the twister–sister ribozyme in solution, starting from the crystal structure reported in Ref. [49••]. The computations propose a conformational change in the catalytic pocket and predict that highly conserved C7 (see labeling in Figure 5f) plays an important role in general acid catalysis either through a direct hydrogen bond to O-5′ at the cleavage step or alternately through mediation of an appropriately positioned hydrated Mg^{2+} cation [65•].

Acknowledgments

The research was supported by NIH 1U19CA179564 (DJP) and NIH P30CA008748 (Cancer Center Core grant to Memorial Sloan-Kettering Cancer Center), by Natural Science Foundation of China grants 91640104 and 31670826, the Fundamental Research Funds for the Central Universities grant 2017QN81010, the new faculty start-up funds from Zhejiang University and the Thousand Young Talents Plan of China (AR) and by Austrian Science Fund FWF P27947 (RM).

Appendix A. Supplementary data

Supplementary material related to this article can be found, in the online version, at http://dx.doi.org/10.1016/j.cbpa.2017.09.017.

References and recommended reading

Papers of particular interest, published within the period of review, have been highlighted as:

- • of special interest
- •• of outstanding interest

1. •• Weinberg Z, Kim PB, Chen TH, Li S, Harris KA, Lunse CE, Breaker RR: **New classes of self-cleaving ribozymes revealed by comparative genomics analysis**. *Nat Chem Biol* 2015, **11**:606-610.

This seminal paper reports on the identification and characterization of twister, twister–sister, pistol and hatchet ribozymes.

2. Prody GA, Bakos JT, Buzayan JM, Schneider IR, Bruening G: **Autolytic processing of dimeric plant virus satellite RNA**. *Science* 1986, **231**:1577-1580.

3. Hutchins CJ, Rathjen PD, Forster AC, Symons RH: **Self-cleavage of plus and minus RNA transcripts of avocado sunblotch viroid**. *Nucleic Acids Res* 1986, **14**:3627-3640.

4. Saville BJ, Collins RA: **A site-specific self-cleavage reaction performed by a novel RNA in Neurospora mitochondria**. *Cell* 1990, **61**:685-696.

5. Perreault J, Weinberg Z, Roth A, Popescu O, Chartrand P, Ferbeyre G, Breaker RR: **Identification of hammerhead ribozymes in all domains of life reveals novel structural variations**. *PLoS Comput Biol* 2011, **7**:e1002031.

6. Martick M, Scott WG: **Tertiary contacts distant from the active site prime a ribozyme for catalysis**. *Cell* 2006, **126**:309-320.

7. Webb CH, Riccitelli NJ, Ruminski DJ, Luptak A: **Widespread occurrence of self-cleaving ribozymes**. *Science* 2009, **326**:953.

8. Rupert PB, Massey AP, Sigurdsson ST, Ferre-D'Amare AR: **Transition state stabilization by a catalytic RNA**. *Science* 2002, **298**:1421-1424.

9. Rupert PB, Ferre-D'Amare AR: **Crystal structure of a hairpin ribozyme-inhibitor complex with implications for catalysis**. *Nature* 2001, **410**:780-786.

10. Fedor MJ: **Structure and function of the hairpin ribozyme**. *J Mol Biol* 2000, **297**:269-291.

11. Cochrane JC, Lipchock SV, Strobel SA: **Structural investigation of the GlmS ribozyme bound to its catalytic cofactor**. *Chem Biol* 2007, **14**:97-105.

12. Klein DJ, Ferre-D'Amare AR: **Structural basis of glmS ribozyme activation by glucosamine-6-phosphate**. *Science* 2006, **313**:1752-1756.

13. Winkler WC, Nahvi A, Roth A, Collins JA, Breaker RR: **Control of gene expression by a natural metabolite-responsive ribozyme**. *Nature* 2004, **428**:281-286.

14. Webb CH, Luptak A: **HDV-like self-cleaving ribozymes**. *RNA Biol* 2011, **8**:719-727.

15. Ke A, Zhou K, Ding F, Cate JH, Doudna JA: **A conformational switch controls hepatitis delta virus ribozyme catalysis**. *Nature* 2004, **429**:201-205.

16. Ferre-D'Amare AR, Zhou K, Doudna JA: **Crystal structure of a hepatitis delta virus ribozyme**. *Nature* 1998, **395**:567-574.

17. Suslov NB, DasGupta S, Huang H, Fuller JR, Lilley DM, Rice PA, Piccirilli JA: **Crystal structure of the Varkud satellite ribozyme**. *Nat Chem Biol* 2015, **11**:840-846.

18. Lilley DM: **The Varkud satellite ribozyme**. *RNA* 2004, **10**:151-158.

19. Breaker RR: **Mechanistic debris generated by Twister ribozymes**. *ACS Chem Biol* 2017, **12**:886-891.

20. •• Jimenez RM, Polanco JA, Luptak A: **Chemistry and biology of self-cleaving ribozymes**. *Trends Biochem Sci* 2015, **40**:648-661.
A comprehensive review on self-cleaving ribozymes covering the literature up to 2015.

21. Lilley DM: **Catalysis by the nucleolytic ribozymes**. *Biochem Soc Trans* 2011, **39**:641-646.

22. Ferre-D'Amare AR, Scott WG: **Small self-cleaving ribozymes**. *Cold Spring Harb Perspect Biol* 2010, **2**:a003574.

23. Scott WG, Martick M, Chi YI: **Structure and function of regulatory RNA elements: ribozymes that regulate gene expression**. *Biochim Biophys Acta* 2009, **1789**:634-641.

24. Cochrane JC, Strobel SA: **Catalytic strategies of self-cleaving ribozymes**. *Acc Chem Res* 2008, **41**:1027-1035.

25. Scott WG: **Ribozymes**. *Curr Opin Struct Biol* 2007, **17**:280-286.

26. • Roth A, Weinberg Z, Chen AG, Kim PB, Ames TD, Breaker RR: **A widespread self-cleaving ribozyme class is revealed by bioinformatics**. *Nat Chem Biol* 2014, **10**:56-60.
Identification of new self-cleaving ribozymes from a compative genomic analysis.

27. Scott WG, Murray JB, Arnold JR, Stoddard BL, Klug A: **Capturing the structure of a catalytic RNA intermediate: the hammerhead ribozyme**. *Science* 1996, **274**:2065-2069.

28. Pley HW, Flaherty KM, McKay DB: **Three-dimensional structure of a hammerhead ribozyme**. *Nature* 1994, **372**:68-74.

29. Blount KF, Uhlenbeck OC: **The structure–function dilemma of the hammerhead ribozyme**. *Annu Rev Biophys Biomol Struct* 2005, **34**:415-440.

30. •• Mir A, Golden BL: **Two active site divalent ions in the crystal structure of the hammerhead ribozyme bound to a transition state analogue**. *Biochemistry* 2016, **55**:633-636.
A key structure of a transition state vanadate analog of the hammerhead ribozyme.

31. • Mir A, Chen J, Robinson K, Lendy E, Goodman J, Neau D, Golden BL: **Two Divalent Metal ions and conformational changes play roles in the hammerhead ribozyme cleavage reaction**. *Biochemistry* 2015, **54**:6369-6381.
This paper provides important insights into nucleotide and divalent cation alignments within the catalytic pocket of the pre-catalytic state of the Rzb hammerhead ribozyme.

32. Chen H, Giese TJ, Golden BL, York DM: **Divalent Metal Ion Activation of a Guanine General base in the hammerhead ribozyme: insights from molecular simulations**. *Biochemistry* 2017, **56**:2985-2994.

33. Harris KA, Lunse CE, Li S, Brewer KI, Breaker RR: **Biochemical analysis of pistol self-cleaving ribozymes**. *RNA* 2015, **21**:1852-1858.

34. •• Ren A, Vusurovic N, Gebetsberger J, Gao P, Juen M, Kreutz C, Micura R, Patel DJ: **Pistol ribozyme adopts a pseudoknot fold facilitating site-specific in-line cleavage**. *Nat Chem Biol* 2016, **12**:702-708.
Refs. [34••,35•] report on pre-catalytic structures of the pistol ribozyme defining residue alignments in the catalytic pocket and discuss the putative role of nucleobases and hydrated Mg^{2+} cations to catalytic activity.

35. • Nguyen LA, Wang J, Steitz TA: **Crystal structure of Pistol, a class of self-cleaving ribozyme**. *Proc Natl Acad Sci U S A* 2017, **114**:1021-1026.
A subsequent structure of the pistol ribozyme validating structural conclusions reported in Ref. [34••].

36. • Kosutic M, Neuner S, Ren A, Flur S, Wunderlich C, Mairhofer E, Vusurovic N, Seikowski J, Breuker K, Hobartner C *et al.*: **A mini-Twister variant and impact of residues/cations on the phosphodiester cleavage of this ribozyme class**. *Angew Chem Int Ed* 2015, **54**:15128-15133.
This paper describes the impact of chemical modifications and divalent cation perturbations on twister ribozyme cleavage chemistry and a 2.6 Å crystal structure.

37. Eiler D, Wang J, Steitz TA: **Structural basis for the fast self-cleavage reaction catalyzed by the twister ribozyme**. *Proc Natl Acad Sci U S A* 2014, **111**:13028-13033.

38. •• Liu Y, Wilson TJ, McPhee SA, Lilley DM: **Crystal structure and mechanistic investigation of the twister ribozyme**. *Nat Chem Biol* 2014, **10**:739-744.
Refs. [38••,39••] report on pre-catalytic structures of the twister ribozyme, while exhibiting important differencs in residue alignments in the catalytic pocket and the putative role of nucleobases and hydrated Mg^{2+} cations to catalytic activity.

39. •• Ren A, Kosutic M, Rajashankar KR, Frener M, Santner T, Westhof E, Micura R, Patel DJ: **In-line alignment and Mg(2)(+) coordination at the cleavage site of the env22 twister ribozyme**. *Nat Commun* 2014, **5**:5534.
See annotation to Ref. [38••].

40. Chen JH, Yajima R, Chadalavada DM, Chase E, Bevilacqua PC, Golden BL: **A 1.9 A crystal structure of the HDV ribozyme precleavage suggests both Lewis acid and general acid**

mechanisms contribute to phosphodiester cleavage. *Biochemistry* 2010, **49**:6508-6518.

41. Golden BL: **Two distinct catalytic strategies in the hepatitis delta virus ribozyme cleavage reaction**. *Biochemistry* 2011, **50**:9424-9433.

42. Ucisik MN, Bevilacqua PC, Hammes-Schiffer S: **Molecular dynamics study of Twister ribozyme: role of Mg(2+) Ions and the hydrogen-bonding network in the active site**. *Biochemistry* 2016, **55**:3834-3846.

43. Neuner S, Kreutz C, Micura R: **The synthesis of 15N(7)-Hoogsteen face-labeled adenosine phosphoramidite for solid-phase RNA synthesis**. *Monatsh Chem* 2017, **148**:149-155.

44. Gebetsberger J, Micura R: **Unwinding the twister ribozyme: from structure to mechanism**. *Wiley Interdiscip Rev RNA* 2016, **8** http://dx.doi.org/10.1002/wrna.1402.

45. • Vusurovic N, Altman RB, Terry DS, Micura R, Blanchard SC: **Pseudoknot formation seeds the Twister ribozyme cleavage reaction coordinate**. *J Am Chem Soc* 2017, **139**:8186-8193.
This paper describes the folding path of twister revealed by smFRET spectroscopy.

46. • Wilson TJ, Liu Y, Domnick C, Kath-Schorr S, Lilley DM: **The Novel Chemical Mechanism of the twister ribozyme**. *J Am Chem Soc* 2016, **138**:6151-6162.
This paper describes the impact of chemical modifications and divalent cation perturbations on twister ribozyme cleavage chemistry.

47. • Gaines CS, York DM: **Ribozyme catalysis with a twist: active state of the twister ribozyme in solution predicted from molecular simulation**. *J Am Chem Soc* 2016, **138**:3058-3065.
Molecular simulations of the active site of the twiser ribozyme starting from the structure reported in Ref. [38••].

48. •• Zheng L, Mairhofer E, Teplova M, Zhang Y, Ma J, Patel DJ, Micura R, Ren A: **Structural-based insights into self-cleavage by a four-way junctional twister–sister ribozyme**. *Nat Commun* 2017, **8**:1180.
Refs. [48••,49••] report on pre-catalytic structures of the twister–sister ribozyme, while exhibiting important differencs in residue alignments in the catalytic pocket and the putative role of nucleobases and hydrated Mg^{2+} cations to catalytic activity.

49. •• Liu Y, Wilson TJ, Lilley DM: **The structure of a nucleolytic ribozyme that employs a catalytic metal ion**. *Nat Chem Biol* 2017, **13**:508-513.
See annotation to Ref. [48••].

50. Li S, Lunse CE, Harris KA, Breaker RR: **Biochemical analysis of hatchet self-cleaving ribozymes**. *RNA* 2015, **21**:1845-1851.

51. Weinberg Z, Nelson JW, Lunse CE, Sherlock ME, Breaker RR: **Bioinformatic analysis of riboswitch structures uncovers variant classes with altered ligand specificity**. *Proc Natl Acad Sci U S A* 2017, **114**:E2077-E2085.

52. Szostak JW: **The narrow road to the deep past: in search of the chemistry of the origin of life**. *Angew Chem Int Ed* 2017, **56**:11037-11043.

53. Sutherland JD: **Studies on the origin of life — the end of the beginning**. *Nat Rev Chem* 2017 http://dx.doi.org/10.1038/s41570-016-0012.

54. Higgs PG, Lehman N: **The RNA world: molecular cooperation at the origins of life**. *Nat Rev Genet* 2014, **16**:7-17.

55. Fedor MJ, Williamson JR: **The catalytic diversity of RNAs**. *Nat Rev Mol Cell Biol* 2005, **6**:399-412.

56. Joyce GF: **The antiquity of RNA-based evolution**. *Nature* 2002, **418**:214-221.

57. Doudna JA, Cech TR: **The chemical repertoire of natural ribozymes**. *Nature* 2002, **418**:222-228.

58. Wochner A, Attwater J, Coulson A, Holliger P: **Ribozyme catalyzed transcription of an active ribozyme**. *Science* 2011, **332**:209-212.

59. Ramakrishnan V: **The ribosome emerges from a black box**. *Cell* 2014, **159**:979-984.

60. Fica SM, Tuttle N, Novak T, Li N-S, Lu J, Koodathingal P, Dai Q, Staley JP, Piccirilli JA: **RNA catalyses nuclear pre-mRNA splicing**. *Nature* 2013, **503**:229-234.

61. Nelson JW, Breaker RR: **The lost language of the RNA world**. *Sci Signal* 2017, **10**:483.

62. Müller UF: **Evolution of ribozymes in an RNA world**. *Chem Biol* 2009, **16**:797-798.

63. Lau MWL, Ferré-D'Amaré AR: **An *in vitro* evolved *glmS* ribozyme has the wild-type fold but loses coenzyme dependence**. *Nat Chem Biol* 2013, **9**:805-810.

64. • Panja S, Hua B, Zegarra D, Ha T, Woodson SA: **Metal ions induce transient folding and activation of the twister ribozyme**. *Nat Chem Biol* 2017, **64**:1109-1114.
FRET and activity assay studies to understand the role of divalent cations in promoting folding and self-cleavage of the *O. sativa* twister ribozyme.

65. • Gaines CS, York DM: **Model for the functional active site of the TS ribozyme from molecular simulation**. *Angew Chem Int Ed* 2017, **56**:13392-13395.
Molecular simulations of the active site of the twister–sister ribozyme starting from the structure reported in Ref. [49••].